Finite volume computational fluid dynamics package for solving convective heat transfer cases

H. Junaidi (corresponding author), D. Henderson, T. Grassie, J. Currie and T. Muneer
Applied Energy Research Group, Napier University, 10 Colinton Road, Edinburgh EH10 5DT, UK
E-mail: h.junaidi@napier.ac.uk

Abstract Computational fluid dynamics (CFD) has brought a step change in the field of flow analysis, particularly in the areas of fluid dynamics and heat transfer, which are intertwined. It has carved a niche in applications where, a decade back, experimentation was the only way forward. This article covers the benchmarking of convective heat transfer cases through the use of CFD software. The cases investigated are common cases of heat transfer involving free convection and one case involving forced convection. The results from CFD analysis are compared with the regressions available for each test case. The two sets of data coincide well, with a percentage difference as low as 0.4%. Information on setting up CFD analysis accurately, particularly for solving problems of natural convection, is also included.

Keywords heat transfer; computational fluid dynamics; free convection; natural convection

Notation

α	thermal diffusivity (m^2/s)
β	thermal expansion coefficient (K^{-1})
δ	boundary layer thickness (m)
δ_t	thermal boundary layer thickness (m)
ρ	density (kg/m^3)
υ	kinematic viscosity (m^2/s)
μ	viscosity ($N.s/m^2$)
Γ	diffusion coefficient
π	angle from the base of the cylinder (degrees)
D	normal distance from heated surface to first cell centroid
g	acceleration due to gravity (m^2/s)
h	convective heat transfer coefficient (W/m^2K)
$\overline{h_x}$	average convective heat transfer coefficient (W/m^2K)
h_{CFD}	convective heat transfer coefficient obtained through CFD (W/m^2K)
h_{exp}	convective heat transfer coefficient obtained through experimentation (W/m^2K)
h_o	enthalpy
h_f	heat transfer coefficient on fluid side
HD	hydraulic diameter
k	thermal conductivity (W/mK)
k_f	thermal conductivity of fluid side (W/mK)

L_c length of the channel
M_w molecular weight
M Mach number (speed of fluid/speed of sound at corresponding temperature)
n local coordinate normal to the wall
Nu Nusselt number ($h\ x\ /\ k$)
Pr Prandtl number (υ/α)
Q rate of heat transfer (W)
R universal gas constant
Ra Reynolds number ($U\ x\ /\ \upsilon$)
Re Rayleigh number ($g\beta\Delta Tx^3/\upsilon\alpha$)
S source term
S_c width of the channel (m)
T temperature (K)
T_o operating temperature (K)
U_∞ free stream velocity (m/s)
u x-direction velocity (m/s)
v y-direction velocity (m/s)
x characteristic length (m)
x_o distance along the wall from starting point of the boundary layer

Introduction

Computational fluid dynamics (CFD) over the last two decades has been of the most rapidly developing areas in engineering. Today, CFD plays a pivotal role in industry by providing robust solutions to flow and heat transfer problems. The technology has found its way into a range of sectors – automotive, aerospace, power generation, environmental, HVAC (heating, ventilation and air-conditioning) and chemical engineering. The popularity of CFD can be attributed to the increase in computational power, which has grown exponentially in the last two decades, thus reducing the processing cost. As a consequence, several general-purpose commercial CFD codes have evolved that can be utilized in the fields mentioned above. However, the software must be set up correctly to yield appropriate results. It should also be noted that CFD is a numerical solution and therefore care should be exercised in problem definition, as incorrect set-up can easily lead to false results or divergence.

Problems in natural convection, of even the simplest form, pose a challenge, due to the intricate nature of the flow. Good regressions are available only for a few elementary cases. In this article, an attempt is made to investigate natural convection problems using CFD. The results obtained were strikingly close to the results obtained through regression, although actual experimental analysis results would have a greater difference because of the radiation losses, which were neglected in all solved cases.

When setting up a CFD problem for free convection, it is imperative to model density as a variable. The differences in density result in buoyant forces, which are responsible for the motion of the fluid. Although all the basic fluid properties (density, viscosity, thermal conductivity and specific heat) are temperature

dependent, in the current study it is only density that has been modelled as a variable. When working with regressions, average values for thermo-physical properties at film temperature are used for calculations. The usage of average values is a reasonable assumption, as the results obtained from them are close to actual values. Therefore, CFD modelling was also done using average constant values for viscosity, thermal conductivity and specific heat. If all these properties were coupled to temperature, the solution would become computationally expensive.

Governing equations

To solve any flow field, the pressure and velocity variables are evaluated by solving continuity and momentum equations. In the case of heat transfer, temperature is an added variable that needs to be taken into consideration, and so the energy equation in such cases is additionally solved. Software based on a finite volume approach utilizes the general transport equation, which reduces the programming effort, as it can be converted into a continuity, momentum or energy equation by changing a single variable (see below). The general transport equation in its integral form [1] is given in equation 1, which is utilized by finite volume solvers:

$$\frac{\partial}{\partial t}\int_V \rho\phi \mathrm{d}V + \oint_A \rho\phi V.\mathrm{d}A = \oint_A \Gamma\nabla\phi.\mathrm{d}A + \oint_A S_\phi \mathrm{d}V \tag{1}$$

Unsteady Convection Diffusion Generation

The general transport equation can be converted into a continuity, momentum (x, y) or energy equation by replacing the variable ϕ with the values given in Table 1.

The Boussinesq model

In solving natural convection flows, faster convergence is achieved if a Boussinesq model is used. The Boussinesq model assumes constant density in all solved equations, except for the buoyancy term in the momentum equation. The density may be represented by a linear function of temperature for small temperature differences and the change in density is related to the thermal expansivity, β [1]:

$$\beta = -\frac{1}{\rho}\left(\frac{\partial\rho}{\partial T}\right)_p \tag{2}$$

If β is approximated by:

TABLE 1 *Values of ϕ in the general transport equation*

Equation	Value of ϕ
Continuity	1
x momentum	u
y momentum	v

$$\beta \cong -\frac{1}{\rho}\left(\frac{\rho_\infty - \rho}{T_\infty - T}\right)_p \tag{3}$$

then,

$$\rho_\infty - \rho \cong \beta\rho(T - T_\infty) \tag{4}$$

In the above expression, density change is linked to temperature change. This would change the momentum equation to:

$$u\frac{\partial u}{\partial x} + v\frac{\partial u}{\partial y} = \beta\rho(T - T_\infty) + v\frac{\partial^2 u}{\partial y^2} \tag{5}$$

Note that the Boussinesq approximation can be used if it meets the following criterion:

$$\beta(T - T_o) \ll 1 \tag{6}$$

where T_o is the operating temperature, or the general temperature of the fluid in the computational domain. This indicates that the approximation can be used only if the temperature variation is not high.

Mesh size

The accuracy of the results obtained from CFD analysis is strongly dependent on the mesh configuration. The mesh size near the boundary is critical, even at low flow speeds. The mesh should be able to resolve both the thermal and the velocity boundary layers. Zhai and Chen [2] have given a detailed explanation of the first 'cell centroid' distance from the boundary for accurate results. When using CFD software based on the finite volume method for analysing natural convection, it is important that the distance of the cell centroid adjacent to the boundary is less than the boundary layer thickness, as higher values lead to larger errors. Thus, to construct the mesh, one needs to know the thickness of the boundary layer in advance. Guidance can be sought from existing analytical solutions for this thickness and thereby to estimate the mesh size. For example, in the case of a free stream velocity, the grid adjacent to the wall for laminar flow should obey equation 7.

$$D\sqrt{\frac{U_\infty}{v x_o}} \leq 1 \tag{7}$$

Equation 7 has been derived from the Blasius solution for flow over a flat plate [1]. Similarly, for the case of natural convection over a vertical wall, the analytical solution shows [3]:

$$\delta_t^4 = \frac{240\left(\frac{20}{21} + \mathrm{Pr}\right)}{\mathrm{Pr}^2\, g\beta\frac{(T_{\mathrm{surf}} - T_\infty)}{v^2}}x \tag{8}$$

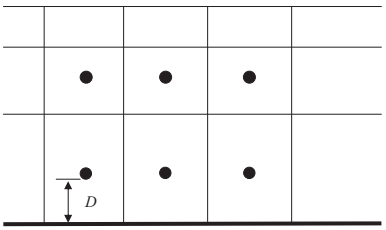

Fig. 1 *The distance of the first cell centroid from the heated surface.*

If the size of the first cell centroid is such that it lies inside the boundary layer, then the error for convective heat transfer is of the order O(D^2) [2]. For the case of natural convection, the calculation error due to the size of the grid is of the order O(D) [2], where D denotes the normal distance of the first cell centroid from the heated surface, as shown in Fig. 1. Once the mesh has met this criterion, any further reduction would not register a notable improvement in the results.

Mesh quality

Alongside mesh size, it is equally important that the shape of the cells is not distorted. For a rectangular or quad mesh, the cells should be ideally square in shape (i.e. all interior angles right angles). This may not always be possible, especially in the case of curved geometries. Similarly, for a triangular mesh – which is usually employed for curved geometries – the cell shape should be as close to an equilateral triangle as possible.

It is also important to understand that the higher the number of cells, the greater is the numerical error. Therefore the total cell count should be kept as low as possible. This can be achieved increasing the cell size in regions of lower gradients. The increase in cell size should not be abrupt, but gradual. An increase with a cell size ratio of 1.1 has been suggested [1].

Domain size

The size of the computational domain for unbounded flows is an important parameter and requires a trade-off: the bigger the domain size, the higher the cell count, and the more computation power is required. Also, if the domain size is kept too small, it will not be able to catch the flow phenomenon completely and will give false results; the computational domain should be kept large enough so that the effects of the geometry on the flow field are not felt at the domain boundaries.

Some authors, such as Baskaran and Kashef [4], suggest that the size of domain can be a multiple of the characteristic height of the flow obstacle in an unbounded flow field. Hu and Wang [5] have estimated the probable error in calculation with the change in size of domain. There are no explicit rules dictating the size of the computational domain; however, results are affected significantly if the extent of the

domain is not appropriate. As a general rule of thumb, 5 hydraulic diameters (HDs) of the geometry are kept upstream and up to 8 HDs downstream within the domain (in case of forced external flows). If the domain is over-sized, then calculations are performed on regions which are unaffected by the flow and as a result the computational effort and time increase unnecessarily.

CFD software environment

For the purpose of the CFD analysis, the popular commercial code Fluent® was used. Geometry creation and meshing (pre-processing) were done using Gambit® from Fluent Inc. For external flow cases, the mesh is kept coarse in regions more distant from the object under study and finer in the regions surrounding it. Where a finer mesh is difficult to generate, the 'grid adaption' feature of the software can be utilized. By running a preliminary analysis, the regions of high temperature and velocity gradients are identified. The existing cells in these regions are marked and subsequently refined using that feature (see Fig. 2). This refinement is carried on until the problem becomes grid independent. The term grid independence implies that any further refinement of the mesh would not have any influence over the results.

For convective heat transfer, Fluent estimates the heat transfer coefficient as [1]:

$$q = h_{\mathrm{f}}(T_{\mathrm{w}} - T_{\mathrm{f}}) \tag{9}$$

In laminar flows, the fluid side heat transfer at walls is computed using Fourier's law applied at the walls. Fluent uses its discrete form:

$$q = k_{\mathrm{f}}\left(\frac{\partial T}{\partial n}\right) \tag{10}$$

where n is the local coordinate normal to the wall.

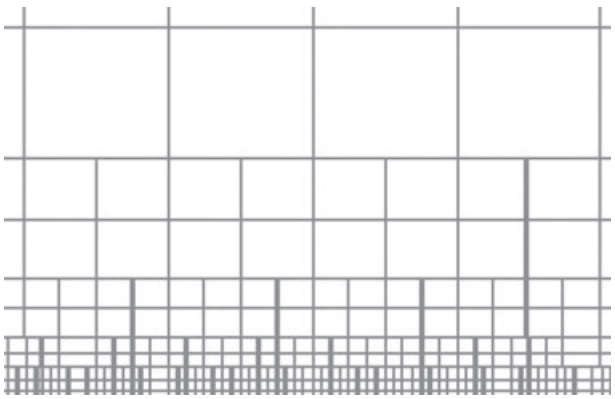

Fig. 2 *Grid refinement using the 'grid adaptation' feature of the software near the boundaries.*

All the cases solved were considered steady-state and two-dimensional, with unit length considered in the depth axis unless stated otherwise. The criteria for residual values for velocities and momentum were reduced to three orders of magnitude (10^{-3}) and for energy up to six orders of magnitude (10^{-6}). This is the minimum criterion for getting quantitative results when using a segregated solver. If higher-order schemes are used for discretizing density, momentum or energy, then the convergence criterion for residuals should be even lower [1].

The PRESTO (pressure staggering option) scheme in Fluent was used for pressure interpolation. Verstag and Malalasekra [6] have given a detailed account of the staggered pressure grid method. PRESTO is recommended for problems with strong body forces, such as gravity forces and pressure gradients, as in high Rayleigh number convection. 'Body force weighted' is another option for pressure discretization provided by Fluent that could be used in cases of high Rayleigh natural convection or highly swirling flows [1].

For density, momentum and pressure discretization, the QUICK (quadratic upstream interpolation for convective kinetics) scheme was used. This gives third-order accuracy results when used with quadrilateral meshes [1]. The flow in all cases solved was considered incompressible, as $M << 1$. Therefore a strong relationship between the density and pressure did not exist. The segregated solver in such cases proves to be more robust and flexible than the coupled solver.

The 'pressure outlet' boundary condition was used to define the domain boundaries in cases of unbounded subsonic flows. This boundary condition requires the specification of static pressure at the outlet boundary, which was set to 0. Where there are large temperature differences inside the domain, density can also be modelled using the ideal gas law. When this option is used, Fluent calculates the density as:

$$\rho = \frac{\frac{P_{\mathrm{op}}}{\mathrm{R}}}{\mathrm{M_w}T} \tag{11}$$

For both the incompressible ideal gas law (IIGL) and the Boussinesq density model, the specification of an operating density significantly improves the convergence rate. It was noted that the IIGL yields results closer to the regressions for higher temperature differences, while the Boussinesq model tends to over-estimate these.

To avoid complexity, only laminar flow was considered in all cases. The Rayleigh number (Ra) evaluated in cases of pure unbounded natural convection was less than 10^8, which suggests buoyancy-induced laminar flow. The transition to turbulence has been said to occur over the range of $10^8 < \mathrm{Ra} < 10^{10}$ [1].

Case studies

Flat plate

The most basic example of forced convective flow is flow over a convective flat plate (see Fig. 3), which can be related to numerous practical flow situations. The

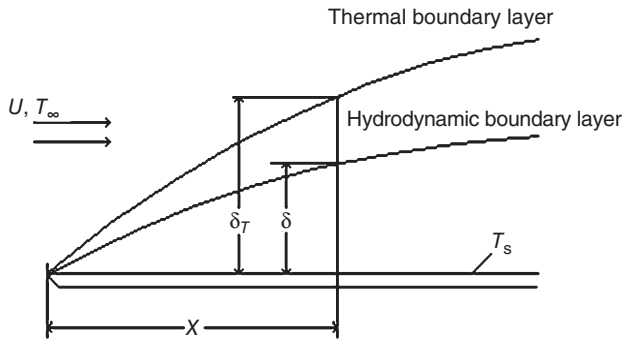

Fig. 3 *Flow over a flat plate.*

TABLE 2 *Properties of air at 308.15 K*

ρ	c_p	μ	υ	k	α	Pr
1.13	1.01	1.88E-05	1.67E-05	2.69E-02	2.37E-05	0.71

Reynolds number: 5.51×10^5.
Nusselt number (average): 438.7.

heat transfer coefficient along the length of the plate decreases with an exponent of –0.5, while the Nusselt number increases by an exponent of 0.5. The value of the average heat transfer coefficient can be given as:

$$\overline{h_x} = \frac{1}{x}\int_0^x h dx \tag{12}$$

The average Nusselt number is given as [7]:

$$\mathrm{Nu}_x = h_x x/k = 0.664\ \mathrm{Re}^{1/2}\ \mathrm{Pr}^{1/3} \quad \mathrm{Pr} \geq 0.6 \tag{13}$$

Test case

Air is considered at a temperature of 26° C flowing over a flat plate of length 2.3 m × 0.2 m at a velocity of 4 m/s. The plate has a uniform surface temperature of 44° C. The film temperature is 308.15 K (35° C), and the properties of air at that temperature are listed in Table 2.

Domain size and mesh

A structured quad (rectangular element) mesh was used. The initial domain shape was a square of dimensions 6.9 m × 6.9 m, which covered 1 HD upstream of the plate and 3 HD perpendicular to the plate. Later, the domain size was reduced to 3.3 m × 3 m (see Fig. 4). This was done on a trial-and-error basis to speed up the solution time and to reduce the number of cells that were inactive (unaffected by the plate) in the solution.

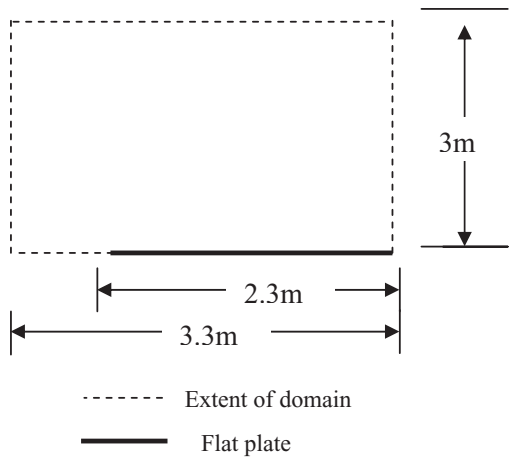

Fig. 4 *The extent of the final computational domain for flow over a flat plate.*

TABLE 3 *Comparison of regression and CFD results for the flat plate test case*

	Regression	CFD	% difference
Q (W)	42.5	42.767	0.628
h (W/m^{2}K)	5.1	5.165	1.27

The size of the first cell adjacent to the plate is critical, as it should be inside the boundary layer. The cell size throughout the domain was kept at 10 mm × 10 mm, apart from at the boundaries, where the mesh was refined to a cell size of 1.25 mm × 1.25 mm. Using equation 1 it can be noticed that a cell size of 10 mm × 10 mm gives $D\sqrt{\frac{U_\infty}{\nu x_o}} = 3.22$, but a cell size of 1.25 mm × 1.25 mm gives D = 0.4, which satisfies the criteria for adequate mesh size set out as equation 7.

Results and validation

The results from the regression calculations are shown in Table 3. It can be seen that they differ very little from the CFD results (by only 0.6% for Q). A graph of the velocity along the vertical distance from the plate surface at 1 m from the leading edge has been plotted in Fig. 5. It can be noticed that the thickness of the velocity boundary layer is less than 0.02 m. The contours of velocity and temperature are shown in Figs 6 and 7, respectively, in which both velocity and thermal boundary layers are evident.

Cylinder

Natural convection around a two-dimensional cylinder has been extensively investigated both numerically and experimentally. Applications in areas such as heat

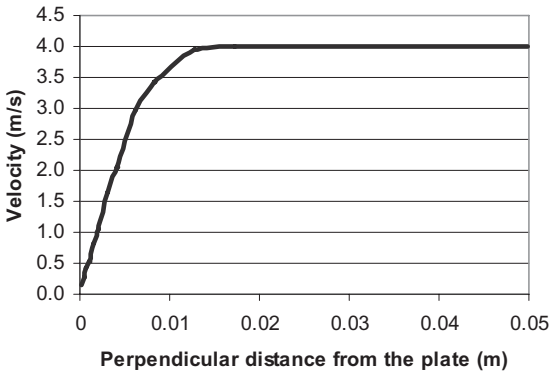

Fig. 5 *CFD results plotting flow velocity against the corresponding height above the plate.*

Fig. 6 *Velocity boundary layer over a flat plate.*

Fig. 7 *Temperature boundary layer over a flat plate.*

exchangers, compact heat sinks, solar dryers and passive solar heaters have promoted the need for better understanding of this phenomenon. Regressions for this case are commonly used to evaluate heat transfer from the pipes or tubes of heat exchangers.

The Nusselt number over the entire circumference can be calculated from the following relation, given by Churchill and Chu [8]:

$$\mathrm{Nu}_D = \left[0.60 + \frac{0.378\mathrm{Ra}_D^{1/6}}{\left[1+\left(\frac{0.559}{\mathrm{Pr}}\right)^{9/16}\right]^{8/27}} \right]^2 \qquad 10^3 < \mathrm{Ra} < 10^{13} \tag{14}$$

Test case

A cylinder of diameter 70 mm is considered, with an outer temperature of the pipe maintained at 100° C. The pipe is exposed to an ambient temperature of 25° C. The film temperature is 335.5 K (62.5° C), and the properties of air at that temperature are shown in Table 4.

Domain size and mesh

The domain was initially modelled considering the complete cylinder (full circle). However, fluctuations in the residual resulted, because of the undulation of the plume generated by hot air that rose from the cylinder, and made it difficult to obtain a fully converged steady-state solution. This problem was alleviated by assuming symmetrical conditions about the vertical axis and modelling only half of the domain.

The cell size throughout the domain was kept at 5 mm × 5 mm, apart from the cylinder boundaries, where it was refined using the grid adaptation feature to a size of 0.125 mm × 0.465 mm. Chouikh *et al.* [9] describe the behaviour of the thickness of the thermal boundary layer with changes in Rayleigh number. At $\mathrm{Ra} = 10^4$ the boundary layer thickness is approximately equal to the cylinder radius. At $\mathrm{Ra} \geq 10^5$ the majority of the flow comes from the side instead of the bottom, but the trend is reversed for smaller Rayleigh numbers. Kitamura *et al.* [10] report separation and transition when the turbulence is beyond $\mathrm{Ra} = 2.1 \times 10^9$, so the assumption of laminar flow is valid.

Results and validation

The values of heat transfer coefficient from the regression and CFD are shown in Table 5. The percentage differences between the regression and the CFD values

TABLE 4 *Properties of air at 335.5 K*

ρ	c_p	μ	υ	k	α	Pr
1.04	1.01	2.01E-05	1.95E-05	2.89E-02	2.78E-05	0.70

Rayleigh number: 1.4×10^6.
Nusselt number: 13.80.

TABLE 5 *Comparison of the regression and CFD results for the cylinder test case*

	Regression	CFD	% difference
Q (W)	94	101.5	7.389
h (W/m^{2}K)	5.7	6.15	7.894

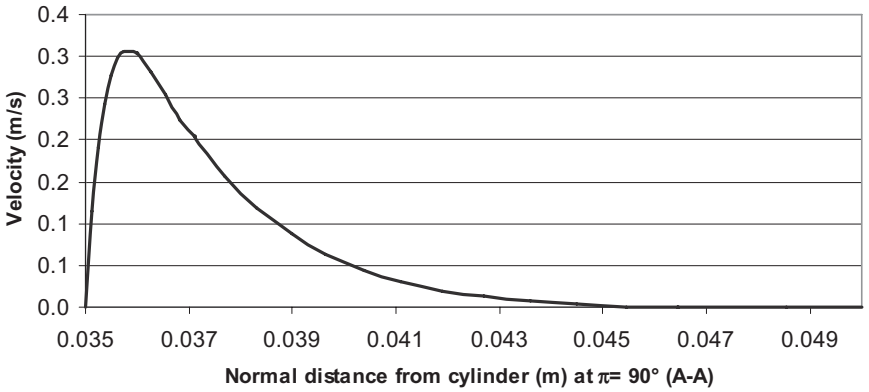

Fig. 8 *CFD results, y-direction velocity plotted against the normal distance away from the cylinder at* $\pi = 90°$.

were over 7%. This is large compared with what was achieved for the flat plat, which can be attributed to the curved nature of the geometry for the cylinder case. The velocity in the *y*-direction is plotted along the imaginary surface A–A (as shown in Fig. 11 below) in Fig. 8. A boundary layer thickness of about 10 mm can be noticed. The results for the velocity and thermal boundary layers over the cylinder from CFD are shown in Figs 9 and 10, respectively. The mesh generated for this case is depicted in Fig. 11.

Vertical channel

Natural convection in a vertical channel has been a widely investigated subject. Applications in electronic cooling, solar energy collectors and nuclear engineering indicate its importance. Bar-Cohen and Rohsenow [11] recommended the following relations for vertical channels (iso-thermal conditions):

$$\mathrm{Nu}_s = \left[\frac{\mathrm{C}_1}{\left(\mathrm{Ra}_s \frac{S_c}{L_c} \right)^2} + \frac{\mathrm{C}_2}{\left(\mathrm{Ra}_s \frac{S_c}{L_c} \right)^{1/2}} \right]^{-1/2} \tag{15}$$

Where C_1 and C_2 are constants, having values of 576 and 2.87 for symmetric iso-thermal plates, S_c is the channel width and L_c its length.

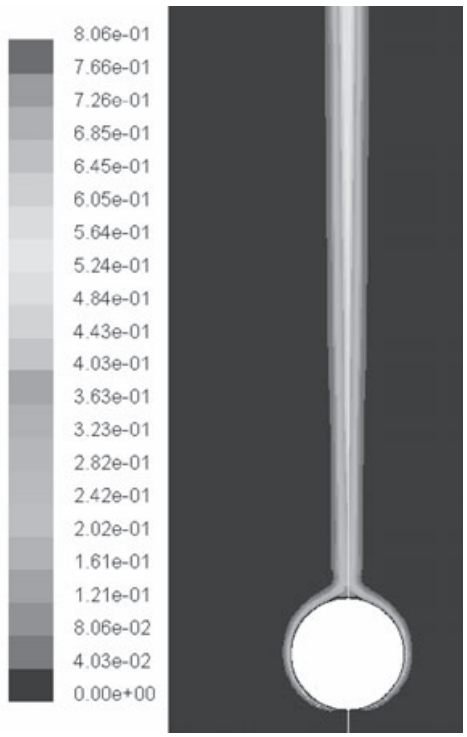

Fig. 9 *Velocity boundary layer in the cylinder test case.*

Test case

Two fins each 1 m long, separated by a distance of 30 mm, are kept at a temperature of 75° C. The ambient air temperature is 16° C. The film temperature is 318.5 K (45.5° C), and the properties of air at that temperature are shown in Table 6.

Domain size and mesh

In order to set up an adequate mesh, it is important to know the thickness of the boundary layer. A crude estimate of the boundary layer thickness is given by [12]:

$$\frac{\delta}{L} \approx \frac{1}{\mathrm{Ra}^{0.25}} \tag{16}$$

where Ra is based on the length of the channel.

As the geometry is regular (i.e. not curved), a quad mesh was used. Since the size of the modelled domain was small, the mesh size throughout the domain was 1 mm × 1 mm. Using equation 8, we get $\delta_t = 0.019$ m. Therefore the mesh was fine enough to resolve the boundary layer. However, a further reduction of mesh was carried out near the boundaries, where the cell size was reduced to 0.25 mm × 0.25 mm. This resulted in a difference of only 0.17% in the value of convective heart transfer.

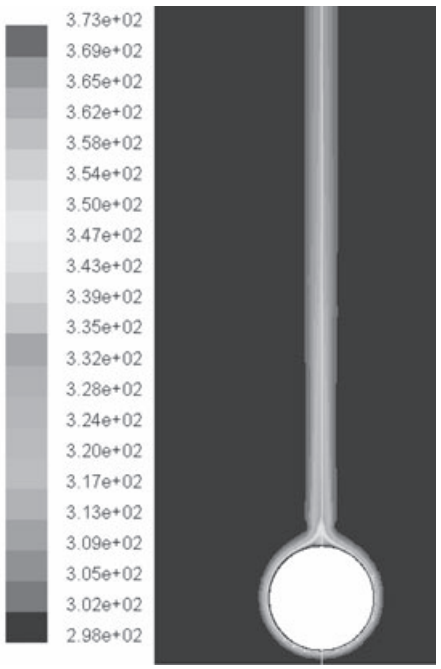

Fig. 10 *Thermal boundary layer and evident hot air plume over the cylinder.*

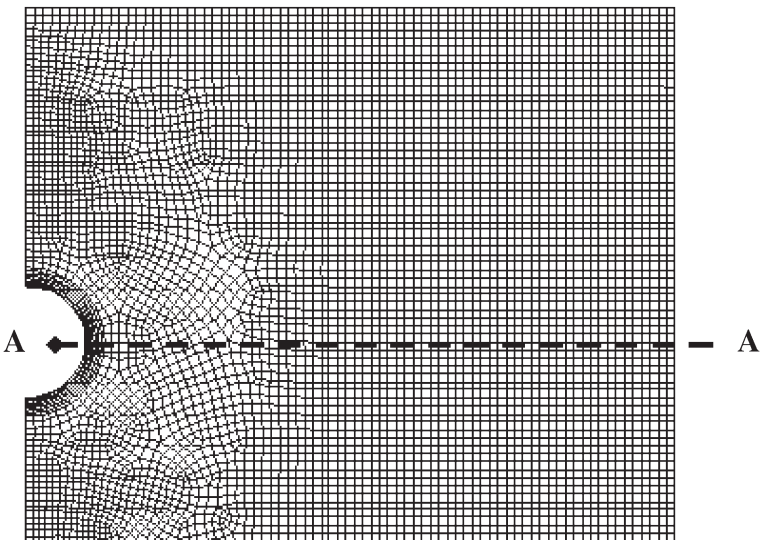

Fig. 11 *Mesh near and away from the cylinder.*

TABLE 6 *Properties of air at 318.5 K*

ρ	c_p	μ	υ	k	α	Pr
1.10	1.01	1.93E-05	1.78E-05	2.77E-02	2.53E-05	0.70

Rayleigh number: 1.09×10^5.
Nusselt number: 4.47.

TABLE 7 *Comparison of regression and CFD results for the vertical channel test case*

	Regression	CFD	% difference
Q (W)	121.6	122.19	0.485
h (W/m^{2}K)	4.12	4.14	0.485

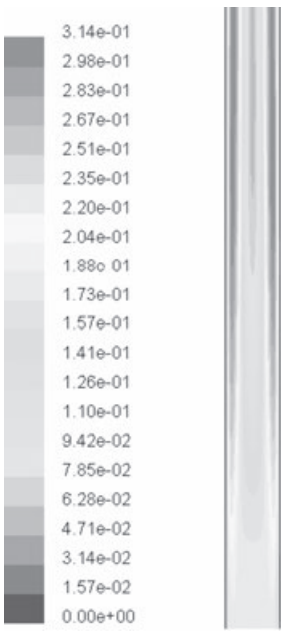

Fig. 12 *Contours of velocity in the vertical channel, showing the development and merging of the velocity boundary layer.*

Results and validation

The results for convective heat transfer using the Bar-Cohen and Rohsenow regression and CFD are shown in Table 7. The percentage difference in regression and CFD values is remarkably low, at under 0.5%. Fig. 12 shows the contours of velocity in the vertical channel.

Vertical cavity

Natural flow in cavities is a topic that has attracted a tremendous amount of interest and is widely used for comparison of numerical codes. Its popularity can be attributed to numerous applications of diverse nature: solar collectors, double-glazed windows, solidification in castings and electronic packaging are just a few examples.

In the case of a two-dimensional vertical cavity, the critical value of the Rayleigh number at which transition to turbulence occurs is 2×10^4, as described by Yin *et al.* [13]. For all entire vertical cavity cases solved using CFD, the value of the Rayleigh number was found to be less than this critical value, and therefore fluid was modelled as laminar.

Several regressions are available covering a range of Rayleigh numbers and geometrical aspect ratios (cavity thickness to cavity length). The current study considered only vertical cavity cases with an aspect ratio above 50. MacGregor and Emery [14] proposed the following relationship by for cavities with a large aspect ratio:

$$\overline{\mathrm{Nu}_L} = 0.42\mathrm{Ra}_L^{1/4}\,\mathrm{Pr}^{0.012}\left(\frac{H}{L}\right)^{-0.3} \tag{17}$$

Test cases

Four cases were solved for the vertical cavity. The details are shown in Table 8. Note that three different geometries for the vertical cavity were tested. The mean temperature in all four cases was 10° C (283 K) and the properties of air at that temperature are listed in Table 9.

Domain size and mesh

An estimate of the non-dimensional boundary layer thickness by Gill [15] is shown in equation 18:

TABLE 8 *Details of four test cases for the vertical cavity*

	Case			
	A	B	C	D
Cavity dimensions	0.6 m × 0.012 m	0.6 m × 0.02 m	1 m × 0.05 m	0.6 m × 0.012 m
In-filled gas	Air	Air	Air	Air
Mean temperature	10° C	10° C	10° C	10° C
Wall temperature	0 and 20° C	0 and 20° C	0 and 20° C	0 and 20° C
Rayleigh number	4.10×10^3	1.90×10^4	2.97×10^5	4.10×10^3

TABLE 9 *Properties of air at 283 K*

ρ	c_p	μ	υ	k	α	Pr
1.24	1.01	1.76E-05	1.44E-05	2.50E-02	2.03E-05	0.71

$$\delta_T \approx 5\mathrm{Ra}^{-0.25} \tag{18}$$

Unlike previous cases, the air cavity is a closed domain problem; therefore the size of the domain is fixed. The cell size was kept at 1 mm × 1 mm, apart from at the boundaries, where a size of 0.25 mm × 0.25 mm was maintained.

Convergence in the case of closed domain convection problems such as the vertical cavity considered here is not readily achieved. As the density is variable, the solver does not have the mass of enclosed fluid beforehand. In such cases, the flow can be modelled in the following ways [1]:

- A transient calculation is initially performed. In this approach, the initial density is computed from the initial pressure and temperature, so the initial mass is known. As the solution progresses over time, this mass will be properly conserved. If the temperature differences in the domain are large, this approach must be followed.
- A steady-state calculation using the Boussinesq model is performed. In this approach, a constant density has to be specified, so the mass is properly specified. This approach is valid only if the temperature differences in the domain are small; if not, the transient approach must be used.

Results and validation

The results were compared with the convective heat transfer coefficient values for various cavity configurations listed in reference [7], which were obtained by experimentation (Table 10). Comparing these with the CFD results in Table 10, it was noticed that the results were an exact match in case A. The biggest difference was only 3.4%, in case D. The results of the velocity contours from the CFD analysis are shown in Fig. 13.

Vertical plate

Natural convection from a vertical plate is an interesting convection study with numerous applications. The most practical situation is that of heat loss from the wall of a room or building. As the buoyant flow is assisted with this geometry configuration, the heat loss in this case is the greater than it is for an inclined or horizontal surface.

The thermal boundary layer can be evaluated using equation 8, and a rough estimate of the thickness of the velocity boundary layer can be estimated using the Pr.

TABLE 10 *Comparison of regression and CFD results for the four vertical cavity test cases*

Case	h_{exp}	h_{CFD}	% difference
A	2.20	2.20	0
B	1.90	1.88	1.05
C	1.80	1.78	1.11
D	1.47	1.42	3.4

Fig. 13 *Contours of velocity in a vertical cavity of dimensions 0.6 m × 0.012 m.*

Churchill and Chu [16] again have provided two relationships for evaluating the Nu over different ranges of Ra.

$$\mathrm{Nu}_L = \left\{ 0.825 + \frac{0.387\mathrm{Ra}_L^{1/6}}{\left[1+\left(\frac{0.492}{\mathrm{Pr}}\right)^{9/16}\right]^{8/27}} \right\}^2, 10^{-1} < \mathrm{Ra_L} < 10^{12} \tag{19}$$

For a lower Rayleigh number range (for higher accuracy), the relationship defined by equation 20:

$$\mathrm{Nu}_L = 0.68 + \frac{0.670\mathrm{Ra}_L^{1/4}}{\left[1+(0.492/\mathrm{Pr})^{9/16}\right]^{4/9}}, 10^{-1} < \mathrm{Ra_L} < 10^{9} \tag{20}$$

Test case

A vertical wall of length 1 m at 350 K is exposed to an ambient temperature of 300 K. The heat loss from this plate is to be determined. The properties of air at the film temperature of 325 K are given in Table 11.

Domain size and mesh

The domain was rectangular, with dimensions 1 m × 0.5 m. One side of this domain represented the vertical wall, at higher temperature. The cell size was kept at 1 mm

Fig. 14 *Cell size can be seen to increase from left to right in the vertical plate test case.*

TABLE 11 *Properties of air at 325 K*

ρ	c_p	μ	υ	k	α	Pr
1.077	1.008	1.96E-05	1.84E-05	0.0282	2.62E-05	0.70

$Ra_L = 3.12 \times 10^9$.

TABLE 12 *Comparison of regression and CFD results for the vertical plate test case*

	Regression	CFD	% difference
Q (W)	172	167.4	2.6
h (W/m^{2}K)	3.4	3.3	2.6

× 1 mm. The cell size increased with the increasing perpendicular distance from the vertical wall, with the ratio 1.1, as shown in Fig. 14.

Results and validation

The results for convective heat transfer using the Churchill and Chu regression and CFD are shown in Table 12. Again, the percentage difference between the regression and CFD values is remarkably low (2.6%). The 'bell shape' profile of the natural convection velocity in a vertical wall, reaching a maximum and dropping again to stagnation, is shown in Fig. 15.

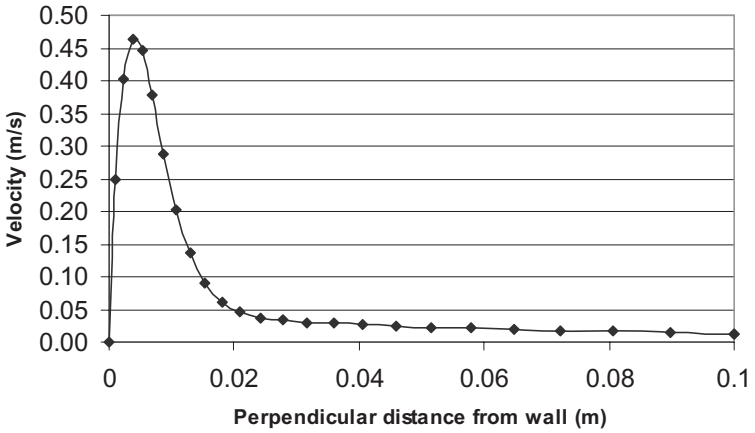

Fig. 15 *CFD results: velocity magnitude at the height centre of the vertical wall.*

Conclusion

CFD is an effective tool not only for visualization but for getting quantitative results for natural convection problems. Setting up the problem accurately in the CFD software is critical, however. The major parameters determining the accuracy of the solution are grid resolution or mesh size, domain extent, choice of density models, discretization schemes and convergence criteria. Each of these parameters has been discussed in detail. Cases for convective flow over a flat plate, cylinder, vertical channel, vertical cavity and vertical plate were solved using CFD. The results obtained were compared with the results obtained by regression. For the case of flow over a flat plate and a vertical channel, very close results were found: the percentage difference with the regression values was only 0.4%. In the case of the horizontal cylinder, the difference was greater, up to 7.3%, because of the curved nature of the geometry. Close results for the vertical cavity (a difference of under 3%) were also observed. It can therefore be ascertained that CFD is an effective tool for solving natural convection problems. It provides deeper insight to the flow and heat transfer phenomena and gives results for numerous points in the domain, information that is not available through regression or experimentation.

Recommendations

The accurate set-up of any problem in CFD software requires a preliminary assessment of many parameters. These include the dimensionless Reynolds, Rayleigh and Prandtl numbers, as well as the boundary layer thickness and temperature variation over the domain. Flow speed should also be noted, as it will dictate the compressibility effects in case of a compressible fluid. The problem to be assessed should also be categorized as two or three dimensional, based on the flow field and the geometry in consideration. Once the mentioned parameters have been reviewed, the

mesh and domain size can be estimated. The criterion for mesh size is linked mainly to the boundary layer thickness, formulae for which have been set out above.

It should be noted, however, that CFD is not a stand-alone application, due to it numerical engine and high probability of inaccurate definition of the problem. The value of experimentation can never be undermined, because of its certainty. CFD, however, has helped significantly in reducing the number of experiments and thus has added robustness to the analysis of flow problems, which otherwise require huge amounts of time and money. Students are encouraged to solve problems relating to natural convection from sources such as textbooks, results for which are known beforehand. Once they achieve a converged solution that matches or is close to the answer, they can then check the same problem or geometry for several 'what if' scenarios, which will enable them to have a better understanding of convective heat transfer and fluid flow behaviour.

References

[1] Fluent Documentation Help, Fluent Europe Ltd (2004).

[2] Zhiqianq Zhai and Qingyan (Yan) Chen, 'Numerical determination and treatment of convective heat transfer coefficient in the coupled building energy and CFD simulation', *Building and Environment*, **39** (2004), 11–14.

[3] J. Lienhard, *A Heat Transfer Textbook*, 3rd edn (Massachusetts Institute of Technology, Cambridge, MA, 1999).

[4] A. Baskaran and A. Kashef, 'Investigation of airflow around buildings using computational fluid dynamics', *Engineering Structures*, **18**(11) (1996), 861–875.

[5] Cheng-Hu Hu and Fan Wang, 'Using a CFD approach for the study of street-level winds in a built-up area', *Building and Environment*, **40** (2005), 617–631.

[6] H. Verstag and W. Malalasekra, *An introduction to Computational Fluid Dynamics: The Finite Volume Method* (Prentice Hall, New York, 1996).

[7] T. Muneer, J. Kubie and T. Grassie, *Heat Transfer – A Problem Solving Approach* (Taylor & Francis, London, 2003).

[8] S. W. Churchill and H. H. S. Chu, 'Correlating equations for laminar and turbulent free convection from a horizontal cylinder', *Int. J. Heat Mass Transfer*, **18** (1975), 1049–1053.

[9] R. Chouikh, A. Guizani, A. El Cafsi, M. Maalej and A. Belghith, 'Experimental study of the natural convection flow around an array of heated horizontal cylinders', *Renewable Energy*, **21**(1) (2000), 65–78.

[10] K. Kitamura, F. Kami-wa and T. Misumi, 'Heat transfer and fluid flow of natural convection around large horizontal cylinders', *Int. J. Heat Mass Transfer*, **42**(22) (1999), 4093–4106.

[11] Bar-Cohen and Rohsenow . . .

[12] FIDAP Documentation Help, Fluent Europe Ltd (2004).

[13] S. H. Yin, T. Y. Wung and K. Chen, 'Natural convection in air layer enclosed within rectangular cavities', *Int. J. Heat and Mass Transfer*, **21** (1978), 307–315.

[14] R. K. Macgregor and A. P. Emery, 'Free convection through vertical plane layers: moderate and high Prandtl number fluids', *J. Heat Transfer*, **91** (1969), 391.

[15] A. E. Gill, 'Numerical boundary layer regime for convection in a square cavity', *J. Fluid Mechanics*, **26** (1966), 515–536.

[16] S. W. Churchill and H. H. S. Chu, 'Correlating equations for laminar and turbulent free convection from a vertical plate', *Int. J. Heat Mass Transfer*, **18** (1975), 1323.

D

AUTHOR QUERY-FORM

Dear Author,

During the preparation of your manuscript for publication, the questions listed below have arisen. Please attend to these matters and return this form with your proof.

Many thanks for your assistance.

Query References	Query	Remarks
1.	Au: Case D is identical to Case A – please check.	

B1